AIChE

Energy Efficient and Controlled Flow Processing Under Microwave Heating by Using a Millireactor–Heat Exchanger

N. G. Patil, A.I.G. Hermans, F. Benaskar, J. Meuldijk, L. A. Hulshof, V. Hessel, and J. C. Schouten
Laboratory of Chemical Reactor Engineering, Eindhoven University of Technology, P.O. Box 513, 5600 MB Eindhoven, the Netherlands

E.V. Rebrov
School of Chemistry and Chemical Engineering, Queen's University Belfast, Stranmillis Road, Belfast, BT9 5AG, U.K.

DOI 10.1002/aic.13713
Published online December 27, 2011 in Wiley Online Library (wileyonlinelibrary.com).

A continuously operated microwave heated millireactor setup has been developed for performing reactions of highly microwave absorbing media in a controlled and energy efficient manner. The setup consists of a tubular reactor integrated with a heat exchanger. A microwave transparent liquid was used as coolant to extract the excess heat from the reaction mixture, thus controlling the temperature of the reaction mixture by avoiding overshoots and subsequent boiling. A reactor-heat exchanger shell and tube unit with a diameter of the inner tube of $3{\cdot}10^{-3}$ m and a shell of $7{\cdot}10^{-3}$ m inner diameter has been manufactured in quartz. The unit size was defined based on simulation with a heat-transfer model for the microwave cavity part. Microwave heating was incorporated as a volumetric heating source term using the temperature-dependent dielectric properties of the liquid. Model predictions were validated with measurements for a range of $0.167{\cdot}10^{-6}$ to $1.67{\cdot}10^{-6}$ m^3/s flow rates of coolant. The outlet temperature of both the reaction mixture and the coolant, were predicted accurately (tolerance of 3 K), and the process window was determined. The model for the reactor part provided the required length of the reactor for a hetero-geneously catalyzed esterification reaction. The predicted conversions, based on the obtained temperature profile in the reactor packed with the catalyst bed, known residence times and kinetics of the esterification reaction, were found to be in good agreement with the experimental results. Efficient utilization of microwave energy with heat recovery up to 20% of the total absorbed microwave power and heating efficiencies up to 96% were achieved. It has been demonstrated that the microwave heating combined with millireactor flow processing provides controlled and energy efficient operation thus making it a viable option for a fine chemical production scale of 1 kg/day (24 h period). © 2011 American Institute of Chemical Engineers *AIChE J,* 58: 3144–3155, 2012
Keywords: Microwave-assisted flow processing, heating efficiency, millireactor-heat exchanger, solid-catalyzed esterification reaction

Introduction

Over the last few decades, there has been a growing interest in the use of microwave heating as an enabling technology to perform high speed organic synthesis with better process selectivity and product yield. Many chemists showed a spectacular increase of the reaction rates in several batch processes in domestic microwave ovens.[1] However, one of the major obstacles for future applications of the microwave technology at industrial scale is scaling-up due to the limited penetration depth of microwaves (few mm) resulting in heating by convection in the center of large batch reactors instead of direct "in core" heating by microwaves.[2] For continuously operated millireactors, the penetration depth problem does not exist and scale-up is done by parallelization.[2–5]

Several authors presented their continuously operated microwave integrated reactor setup for performing a diversity of chemical reactions. Although they reported an increase in yield,[4] the presence of hot spots[6–8] and an increase of the reaction rate,[9] there was a lack of insight into the actual amount of transferred energy which is important for efficient scale-up. Esveld et al.[10,11] calculated the efficiency of microwave heating to be 37%, while the remaining energy was mostly lost as a result of indirect heating of the support and the surrounding air. In this case, use of a multimode microwave cavity, due to its uneven electromagnetic field distribution, resulted in a low reproducibility and efficiency.[12,13] Patil et al.[14] showed that monomode microwave applicators providing a well defined electric field pattern can be a suitable option for transforming fine chemical batch processes into a continuous operation with higher efficiency and reproducibility.

Accurate temperature measurements are crucial for a proper interpretation of microwave heating effects. However,

Correspondence concerning this article should be addressed to J. C. Schouten at J.C.Schouten@tue.nl.

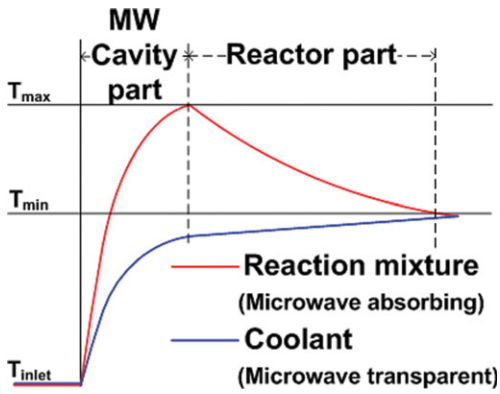

Figure 1. Schematic representation of temperature profiles in an integrated reactor-heat exchanger for flow processing with microwave heating.

[Color figure can be viewed in the online issue, which is available at wileyonlinelibrary.com.]

several articles described indirect methods of temperature measurements such as infrared detectors.[3,15–17] Such indirect methods resulted in measuring the temperatures of the reactor wall instead of the reaction medium, subsequently leading either to alleged microwave effects or to poor understanding of the temperature distribution. However, temperature measurements can be done more accurately by using a fiber-optic sensor.[8–10] These sensors inserted in the reaction mixture, measure the temperature directly and are microwave transparent and do not disturb the microwave field.[18]

A completely thermally insulated continuous flow recycle monomode microwave reactor is reported by Chemat et al.[4] This configuration allows high-microwave absorption due to improved interaction between the microwave field and the reaction mixture.[13,16] The high-energy intensity of the focused microwaves, however, makes an efficient and controlled operation impossible especially when a strong microwave absorbing solvent is used. Some of the proposed continuous flow reactor systems suggest use of a dead load to extract the excess of microwave energy for avoiding runaway.[3,15] A tubular reactor integrated with a heat exchanger can provide a solution in such cases where a cocurrently flowing microwave transparent (nonpolar) solvent is used as coolant to avoid overheating of the reaction mixture (Figure 1). Additionally, because of cocurrent operation rather than counter current, the excess of heat can also be used to maintain the reaction temperature over longer lengths of a continuously operated tubular reactor outside the microwave cavity.

In this article, we present an integrated heat exchanger reactor system for efficient and controlled flow processing of highly microwave absorbing reaction media. Esterification of ethanol and acetic acid around 343 K was chosen as a model reaction (Scheme 1). Toluene, being a microwave transparent solvent, was used as coolant. To achieve insight into the temperature profiles the reactor-heat exchanger system was divided in two parts that is, the microwave cavity and the reactor downstream the cavity (Figure 2). Heat-transfer models were developed to describe the temperature profiles for the reaction mixture and the coolant in both parts. Both models were validated experimentally while depicting the controllability and efficiency of operation.

Theoretical modeling

In the microwave cavity part of the proposed integrated reactor-heat exchanger, microwave energy absorbed by the reaction mixture gets distributed between the reaction mixture, coolant and heat losses to the surroundings. Note that the reaction mixture being the only microwave absorbing component takes up all the microwave energy present in the cavity which subsequently gets transferred to the nonabsorbing coolant by conduction and convection. Part of the energy absorbed by the coolant gets lost to the surroundings by natural convection. In the reactor part the heat lost by the reaction mixture is equal to the energy gained by the coolant. The overall energy balances for both parts are schematically depicted in Figure 2.

Although the reactor part is thermally insulated, the reaction mixture cools down over the reactor length. However, the warm coolant here acts like an extra insulation medium, allowing the reaction mixture to cool gradually. This axial temperature profile was determined by modeling the heat transfer in the fixed-bed reactor part. Conversion as a function of the axial position can be calculated by including temperature-dependent kinetics of the reaction and by solving standard fixed-bed equations.[19]

Two Dimensional (2-D) heat-transfer model for the microwave cavity part

A pseudo 2-D model was developed in COMSOL multiphysics for the microwave cavity part to estimate the dimensions of the reactor and the range of operating conditions (Figure 7). Microwave heating was incorporated as a volumetric heating term in the micro heat balance. It was based on the temperature-dependent dielectric properties of the reaction mixture (see the subsection on volumetric heating). The physical properties of strongly microwave absorbing ethanol, being in excess, were used as reaction mixture properties (microwave absorbing liquid), and those of microwave transparent toluene were used as coolant properties (Table 1).[20]

The tube and shell walls of the heat exchanger were modeled with the physical properties of quartz (k =1.38 W/m.K). The hydrodynamics of laminar flow was described by the incompressible Navier-Stokes equations (Eq. 1). A standard microheat balance (Eq. 2) was used to determine the temperature profiles in the liquids, while heat transfer to the solid wall was used as a boundary condition in solving the microheat balance in the microwave cavity. The quadrangle element was used as the basic element type for the mesh (mapped mesh parameters), consisting of 4,560 elements. The direct linear system solver (UMFPACK) was used to

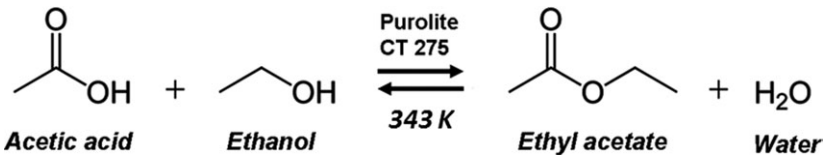

Scheme 1. Ester formation from acetic acid and ethanol.

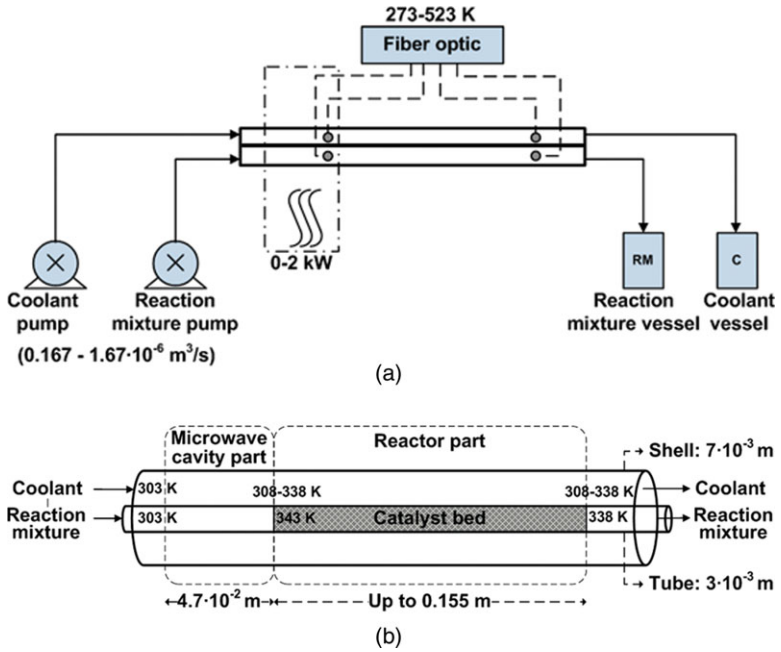

Figure 2. (a) Process flow diagram, and (b) schematic of the integrated reactor-heat exchanger system with process details, divided into the microwave cavity part and the reactor part, including overall energy balances.

[Color figure can be viewed in the online issue, which is available at wileyonlinelibrary.com.]

determine the temperature profiles of the reaction mixture and the coolant in the microwave cavity part

$$\rho\frac{\partial u}{\partial t}+\rho(u\cdot\nabla)u=\nabla\cdot\left[-pI+\mu\left(\nabla u+(\nabla u)^T\right)\right]+F \quad (1)$$

$$\rho C_p\left(\frac{\partial T}{\partial t}+u\cdot\nabla T\right)=\nabla\cdot(k\nabla T)+Q \quad (2)$$

Assumptions and constraints

Heat transport was computed with the following assumptions:

- The reactor material (quartz), and the coolant (toluene) are microwave transparent.
- The volumetric heating source is uniform in the radial and axial directions of the load.
- Considering laminar flow, the heat-transfer coefficients are averaged over the length of the microwave cavity.

The dimensions of the microwave cavity part had the following restrictions:

- The length of the microwave cavity is $4.7\cdot10^{-2}$ m; within this length the temperature of the reaction mixture has to increase from room temperature that is, 303 K to 343 K.
- Outer diameter of the shell cannot be larger than 9 mm due to physical limitations of the setup.

Table 1. Physical Properties of Reaction Mixture (Ethanol), Coolant (Toluene) and Walls (Quartz)

Property	Ethanol	Toluene
Thermal conductivity [k, W/(m.K)]	0.167	0.14
Density [ρ, kg/m^3]	842.76	866.9
Heat capacity [C_p, J/(kg.K)]	2359.34	1698.5
Viscosity [μ, Pa.s]	$1.201\cdot10^{-3}$	$0.548\cdot10^{-3}$

- Minimum required space between the shell and tube and the minimum diameter of the inner (reactor) tube is 1.1 mm to facilitate insertion of fiber-optic sensors for validation experiments.

Heat-transfer coefficients

With fully developed flow of an incompressible fluid through a circular duct and constant heat flux to the wall, the Nusselt number can be assumed to be 4.36.[19] By using this Nusselt value and the thermal conductivity of ethanol (k =0.167 W/m.K), the heat-transfer coefficient of the reaction mixture (h_{RM}) was calculated to be 243 W/m^2.K. The Nusselt value is dependent on the ratio of the inner and the outer diameter for laminar flow through the annular region of the coaxial circular duct,[21] and was found to be 8.1, assuming constant heat flux to the wall. By using this Nusselt value and the thermal conductivity of toluene (k =0.14 W/m.K), the heat-transfer coefficient of the coolant (h_C) was calculated to be 378 W/m^2.K. The heat-transfer coefficient for the heat losses to the surroundings by natural convection (h_{surr}) was assumed to be 10 W/m^2 K. Heat transfer in the microwave cavity was assumed to be in series, where heat was transferred from the reaction mixture to the coolant and from the coolant to the surroundings. Thus, the overall heat-transfer coefficients at the reaction mixture boundary (U_{RM}) and coolant boundary (U_C) were calculated to be 154.0 W/m^2.K and 11.7 W/m^2.K, respectively.

Volumetric heating

Microwave heating was incorporated as a volumetric heating term using the equation of Metaxes and Meredith,[22] see Eq. 3

$$Q_{MW}=2\pi f\varepsilon_0\varepsilon''E^2V_R \quad (3)$$

The dielectric loss (ε'') in Eq. 3 depends on the temperature. This dependency was determined by using a dielectric

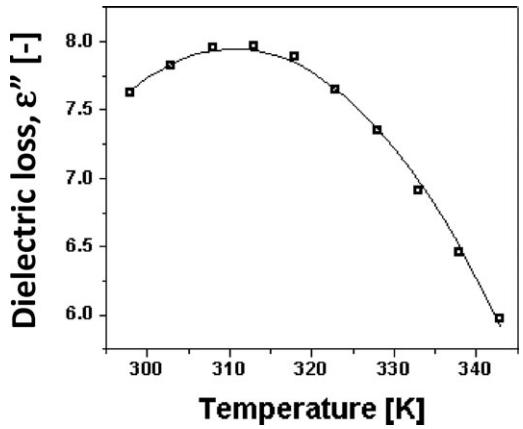

Figure 3. Dielectric loss (ε'') of ethanol as a function of the temperature.

Symbols: experimental values; Line: polynomial fit.

probe kit and network analyzer,[14] resulting in Eq. 4 based on experimental data in Figure 3

$$\varepsilon'' = -1.9328 \cdot 10^{-3}T^2 + 1.2005T - 1.7843 \cdot 10^2 \quad (4)$$

The electric field intensity (E) at the reactor opening (Figure 4) was empirically determined as a function of the applied power (Q_{cav}, Eq. 5) for small temperature gradients ($\leq$ 5 K), i.e., no heat loss to the surroundings (Q_{loss} =0), and constant dielectric properties (ε' and ε'') of the used solvent. This resulted in the empirical Eq. 5 based on the data in Figure 4

$$E = 1.150 \cdot 10^{-3}Q_{\text{cav}}^3 - 4.673 \cdot 10^{-1}Q_{\text{cav}}^2 + 1.043 \cdot 10^2 Q_{\text{cav}} + 2.334 \cdot 10^3 \quad (5)$$

Equations 4 and 5 were inserted as scalar expressions in the respective subdomains for instantaneous quantification of the volumetric heating term in the microheat balance.

1-D Heat-Transfer Model for the Reactor Part

The design of the reactor, was aimed at keeping the temperature of the reaction mixture as long as possible constant and at least between 343 and 338 K ($T_{\max}$ and T_{min}, respectively, see Figure 1). Although the esterification reaction was slightly exothermic (−2,400 J/mol, Appendix A), it was necessary to insulate the heat exchanger to avoid heat losses to the surroundings. To predict the axial temperature profiles in the reaction part after the microwave cavity, Polymath (Version: 6.10) was used. The temperatures were described by two-coupled 1-D differential equations described in following subsection on energy balances.

Assumptions and constraints

- Heat is transferred through the wall of the reactor.
- Perfect radial mixing, i.e., no radial temperature gradient in the packed-bed reactor.
- Heat of reaction is negligible.
- No heat loss to the surroundings.

Energy balances

The energy balances for a plug flow reactor in terms of molar flow rates are presented in Eq. 6 and Eq. 7.[19]

$$\frac{dT_{RM}}{dL} = A_{RM}\frac{U_{RM}^*(T_C - T_{RM})}{m_{RM}^{\bullet}C_{P-RM}} \quad (6)$$

Similarly, the coolant temperature varied over the length of the reactor part

$$\frac{dT_C}{dL} = A_C\frac{U_C^*(T_{RM} - T_C)}{m_C^{\bullet}C_{P-C}} \quad (7)$$

The coupled differential equations were simultaneously solved using polymath for a range of coolant flow rates. The overall heat-transfer coefficient terms (U_{RM}^* and U_C^*) were used as fitting parameters.

Modeling of the Chemical Reaction

The length of the reactor part, giving temperatures between 343 and 338 K ($T_{\max}$ and $T_{\min}$) was determined from the temperature profiles of the liquids given by the heat transfer model of the reactor part. Subsequently, the conversion is determined by the amount of solid catalyst, varying with the length of the reactor part, and can be described by the standard design equations for a isothermal packed bed reactor with a pseudo first-order irreversible reaction (Eq. 8).[19] Thus, the heat-transfer model of the reactor part as described in earlier section was further extended by incorporating Eq. 9 for chemical reaction modeling to predict conversions

$$F_v^A dC_A = r_A' = k_{(T)}^v C_A dW \quad (8)$$

$$X = \left(1 - \left(\exp\left(\frac{k^v}{F_v}W\right)\right)^{-1}\right)100\% \quad (9)$$

Constant pressure was assumed as Ergun equation predicted a pressure drop of $1.8{\cdot}10^4$ Pa for the longest packed bed of 0.155 m (Appendix B),[19] by which (a) from batch

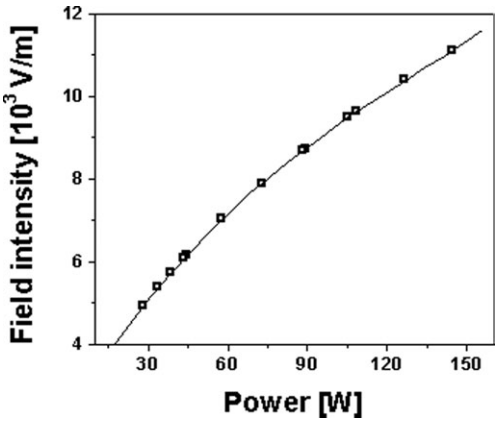

Figure 4. Electric field intensity as a function of microwave power.

Symbols: experimental values; Line: polynomial fit.

experiments, the volumetric reaction rate constant was found to be $3.3 \cdot 10^{-3}$ s^{-1} at 343 K (Appendix C). Based on the Arrhenius equation, the activation energy and the pre-exponential factor were calculated to be 53.5 kJ/mol and $2.6 \cdot 10^{6}$ s^{-1}, respectively. The heat produced by the reaction for 10% conversion was found to be negligible at $4.9 \cdot 10^{-2}$ W (Appendix A). Therefore, the reaction rate coefficient was assumed to be constant with respect to temperature (343 K) by ignoring the heat of reaction.

Experimental Setup and Procedures

Figure 2 schematically illustrates the process details of the integrated reactor-heat exchanger system. Both the liquids, reaction mixture and coolant, while flowing through the integrated reactor-heat exchanger, first enter the microwave cavity part where the reaction mixture is heated directly by the microwaves and excess of the microwave energy gets transferred to the coolant by heat transfer. At the outlet of the microwave cavity part, the reaction mixture at the reaction temperature, i.e., 343 K and the coolant with similar elevated temperature enter the reactor packed with catalyst over the predetermined reactor length.

Equipment and chemicals

The microwave setup was designed and developed in collaboration with Fricke und Mallah GmbH (Figure 5). The system consisted of a single-mode microwave cavity operating at a frequency of 2.45 GHz with adjustable power settings up to 2 kW.[14] Process control and data acquisition over the entire setup was performed via the labVIEW program. The reflected power was recorded by using a detector diode on an isolator. The power available in the cavity could be calculated with an accuracy of approximately 10%.

The reactor-heat exchanger consisted of two quartz tubes (Figure 2), connected with T-junctions for liquid supply and temperature measurement ports. Heat-transfer modeling (see previous section) results revealed that the most suitable diameter for the inner (reactor) tube was $3 \cdot 10^{-3}$ m with a wall thickness of $5 \cdot 10^{-4}$ m, while the shell diameter is $7 \cdot 10^{-3}$ m with a wall thickness of $1 \cdot 10^{-3}$ m. Teflon spacers were used to support the reactor-heat exchanger in axially centric position and also to prevent heat losses to the metal supports. An insulation foam was used for insulating the reactor part outside the microwave cavity. Gilson HPLC pumps (flow range: $8.33 \cdot 10^{-9}$ to $2.5 \cdot 10^{-6}$ m^3/s) were used to supply the reaction mixture and the coolant to the inner (reactor) tube and the shell, respectively. Fiber-optic sensors, type OTG-A, supplied by OpSense® were used to record the temperature inside the reactor tube and the surrounding shell.

Experimental Procedures

Two types of experiments were performed; i.e., physical experiments for the determination of temperature profiles inside the microwave cavity and reactor, and chemical experiments for determining the conversion.

Physical experiments: determining the temperature profiles of the reaction mixture and coolant

The temperature profiles in the microwave cavity and in the reactor part are necessary to validate both heat-transfer models (see previous section). Before starting the physical experiments, the quartz reactor-heat exchanger was placed at a fixed position in the reactor opening of the microwave cavity. After focusing the microwaves on the reaction mixture and placing the fiber-optic sensors in the required position, the temperature measurements were ran for few minutes after reaching the steady state. The temperature was recorded against time by using the labVIEW program. The reaction mixture had a steady state within a few seconds, but a few minutes (ca. 300 s) of run time was needed to reach the steady-state temperature of the coolant because conduction and convection were not as fast as heating by the microwaves. Four fiber-optic sensors were simultaneously used for experimental determination of temperature profiles in the reactor tube and shell over the whole length (every $1 \cdot 10^{-2}$ m) of the microwave cavity and reactor parts.

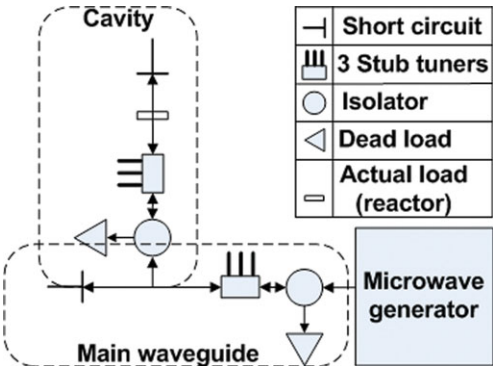

Figure 5. Schematic view of microwave setup with microwave energy flow.

Arrows showing directions of wave propagation. [Color figure can be viewed in the online issue, which is available at wileyonlinelibrary.com.]

Chemical experiments: determining the conversion

In this study, the heterogeneously catalyzed esterification of acetic acid (99.8%, Sigma Aldrich) and ethanol (99.8%, Sigma Aldrich) was chosen as a model reaction (Scheme 1).[23] In order to increase the conversion for this equilibrium-limited reaction, a five-fold excess of ethanol was chosen because of its polarity and enhanced microwave absorption. The reaction was performed between 338 and 343 K (Figure 1). The maximum temperature was set at 343 K to avoid boiling of ethanol.[4] The catalyst, an acidic ion exchange resin (CT 275, Purolite®) with average particle diameter of $750 \cdot 10^{-6}$ m, was dried before use for two days at room temperature. The experiments were performed by packing the predetermined length of the reactor part with catalyst. The reaction mixture flowing through the microwave cavity got heated to the reaction temperature and entered the catalyst bed for actual reaction before leaving the system toward the collection vessel. Samples were taken over time and analyzed by gas chromatography (GC) to determine the conversion. The samples for GC analysis were diluted with methyl isobutyl ketone (99.8%, Sigma Aldrich) with a dilution of 10 wt % to lower the concentrations of ethanol and acetic acid to precisely determine the concentrations of the reaction components. From the GC-results, the conversion of acetic acid, the limiting reactant, was calculated over time. After a single pass through the catalyst bed, the conversion was below 0.5%, resulting in large errors by GC-analysis and, therefore, the reaction mixture was recycled. During these recycles, the collection vessel of the reaction mixture was stirred firmly at 500 rpm.

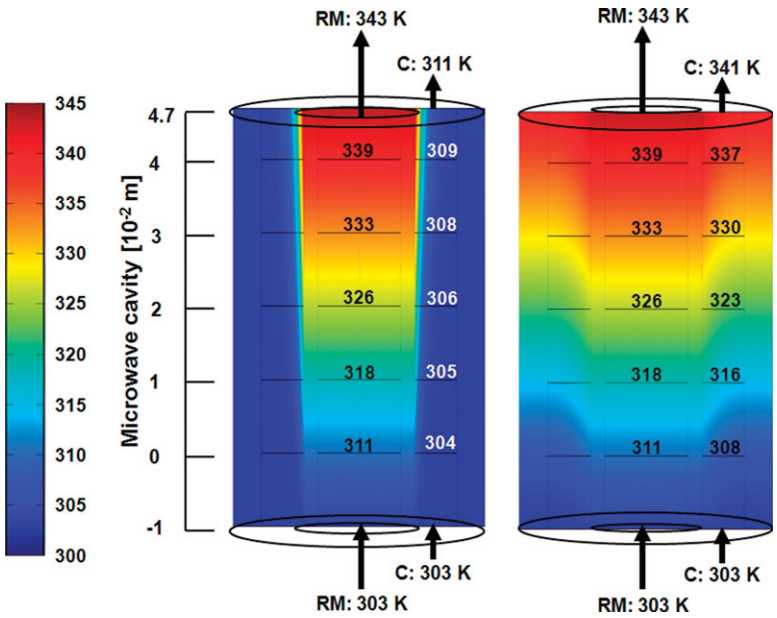

Figure 6. Modeling results for two different flow rates of coolant, $8.33{\cdot}10^{-7}$ m^3/s (a) and $8.33{\cdot}10^{-9}$ m^3/s (b), at constant flow rate of the reaction mixture: $6.66{\cdot}10^{-7}$ m^3/s, available power: 163 W.

Numbers on several internal boundaries show temperature at the respective boundary. RM: reaction mixture, C: coolant. [Color figure can be viewed in the online issue, which is available at wileyonlinelibrary.com.]

Results and Discussion

The heat-transfer models, developed for the microwave cavity and reactor sections and the model of the chemical reaction were validated by experiments. The experimental results as well as the results of the model predictions are discussed in detail in the following sections.

Validation of the temperature profile in the microwave cavity part

The obtained model predictions by the 2-D heat-transfer model for the microwave cavity part are shown in Figure 6. The modeling results demonstrated that the flow rate of the coolant has a negligible influence on the outlet temperature of the reaction mixture even at 100 times increase in the coolant flow rate (Figure 6). Thus, controlling the outlet temperature of a highly microwave absorbing reaction mixture by varying the flow rate of the coolant was not possible in the chosen reactor-heat exchanger geometry. There can be two reasons for this, i.e., first, the limited heat-transfer area due to the design restrictions of the reactor-heat exchanger and, second, the time constant for microwave heating is much lower than the time constant for convective heat transfer to the coolant. However, the results of the model predictions demonstrate that the outlet temperature of the reaction mixture could be well controlled by adapting the flow rate of the reaction mixture and the applied microwave power. The experimental results demonstrated that at a distance of $1{\cdot}10^{-2}$ m before the microwave cavity, the reaction mixture and the coolant were already heated to a temperature considerably above room temperature (Figure 7, data point at 0 m), due to the propagation of microwaves outside the cavity in the direction of the liquids inlet. Therefore, the volumetric heating source in the heat transfer model was also added for this $1{\cdot}10^{-2}$ m making the microwave cavity $1{\cdot}10^{-2}$ m longer than its actual size of $4.7{\cdot}10^{-2}$ m (Figures 6 and 7).

Inside the cavity, a linear increase of temperature for both the reaction mixture and the coolant was predicted by the model, while an exponential rise was observed experimentally (Figure 7). The model predicted a linear temperature increase in both the liquids because microwave heating was incorporated as a volumetric heating source with a constant and uniform field distribution over the entire load rather than taking into account instantaneous interaction of the microwaves with varying applied load (i.e., changing dielectric constant, ε'). Note that this simplified modeling of the microwave heating process has previously proven to be useful in predicting temperature profiles of the reaction mixture.[3] A hot spot was observed for the reaction mixture around $2{\cdot}10^{-2}$ m inside the microwave cavity (Figure 8). The temperature of this hot spot was higher when no coolant was present in the shell of the reactor-heat exchanger (Figure 8). Thus, the coolant plays the role of avoiding overheating of the reaction mixture by taking up excessive microwave energy. Further investigations are in progress to understand the hot spot formation inside the microwave cavity especially with a focus on the field distribution.

Although the axial temperature profile of the reaction mixture in the cavity is not completely understood, the model predicted the outlet temperatures with an accuracy of $\pm$ 3 K; therefore, the model was further used to determine the process window (Figure 9). The graph represents the power needed in the cavity to achieve an outlet temperature of 343 K at the end of the microwave cavity part for different flow rates of the reaction mixture. The flow rate of the coolant was kept constant at $8.33{\cdot}10^{-9}$ m^3/s for all these simulations. In the most favorable situation for the esterification reaction, the flow rate of the reaction mixture should be as low as possible to achieve a long residence time for conducting the reaction in the reactor part. However, in this case a very low-microwave power had to be applied (Figure 9). Stability of operation restricted the continuous flow setup to a minimum microwave power of 155 W. As a result the flow rate of the reaction mixture had to be adapted to $6.66{\cdot}10^{-7}$ m^3/s to achieve an outlet temperature of 343 K (Figure 9). Accurate

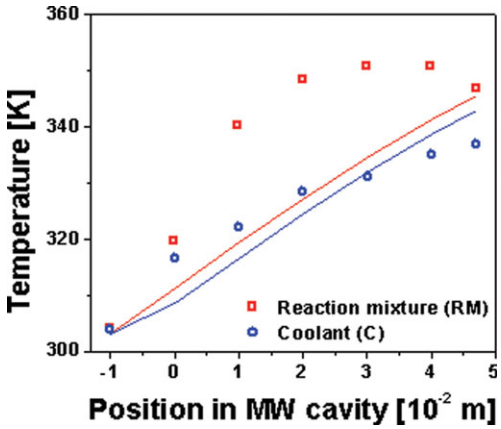

Figure 7. Model vs. experimental data, showing temperature profiles of the reaction mixture (RM), and the coolant (C) inside the microwave cavity.

Symbols: experimental results; Lines: model predictions. Flow rates RM: $6.66{\cdot}10^{-7}$ m^3/s, C: $8.33{\cdot}10^{-9}$ m^3/s, available power: 163 W. [Color figure can be viewed in the online issue, which is available at wileyonlinelibrary.com.]

knowledge of the microwave power level in the setup was necessary for further calculation of the microwave heating efficiency.

Validation of the Temperature Profile in the Reactor Part

During the experiments, the inlet temperature of the reactor part was not always exactly 343 K ($\pm$ 2 K) due to differences in the reflective microwave power. So, for validation of the 1-D heat-transfer model of the reactor part, the inlet temperatures in the model were adapted to the experimental results. The flow rate of the reaction mixture was kept constant at $6.66{\cdot}10^{-7}$ m^3/s in these experiments (see previous section). The flow rate of the coolant was varied between 8.33 and $250{\cdot}10^{-8}$ m^3/s. A higher coolant flow rate, having a lower coolant temperature at the end of the microwave cavity part, resulted in a larger driving force for heat exchange in the reactor part. This influenced the axial temperature profiles of both reaction mixture and coolant in the reactor part. Heat exchange started at the outlet of the microwave cavity part. So $x = 0$ in Figure 10 is the inlet of the reactor part and the outlet of the microwave cavity part.

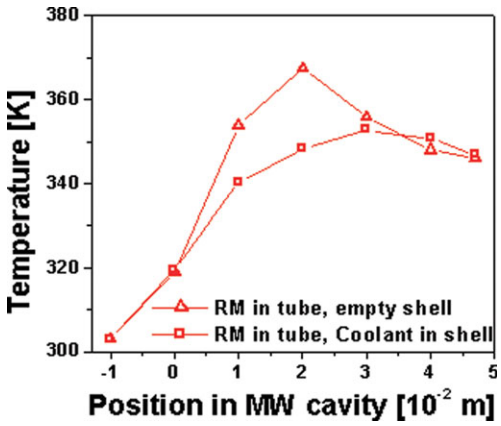

Figure 8. Experimentally observed temperature profile of the reaction mixture (RM) with (square) and without (triangle) coolant flow in the shell.

Flow rate RM: $6.66{\cdot}10^{-7}$ m^3/s, C: $8.33{\cdot}10^{-9}$ m^3/s, available power: 150–160 W. [Color figure can be viewed in the online issue, which is available at wileyonlinelibrary.com.]

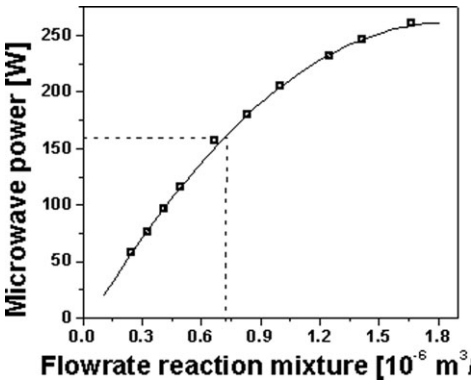

Figure 9. Process window for the applied microwave power and reaction mixture flow rate to achieve 343 K at the outlet of the microwave cavity part.

Flow rate of the coolant: $8.33{\cdot}10^{-9}$ m^3/s; Symbols: modeling points, Line: a guide to the eye.

The heat-transfer model predicted the temperature profile of the reaction mixture quite accurately (Figure 10). Deviations in the model predictions from the experiments could be due to errors in the experimental measurements and the different reflective powers during the experiment. The predictions were less accurate for higher flow rates of the coolant, probably because the heat-transfer coefficient can be a function of the flow rate in this case, while it was assumed to be constant in the model.

For the esterification reaction, a near isothermal operation with the temperature of the reaction mixture between 338 and 343 K was required. Note that the flow rate of the coolant determined the length of the reactor part for reaction since its temperature at the end of the microwave cavity

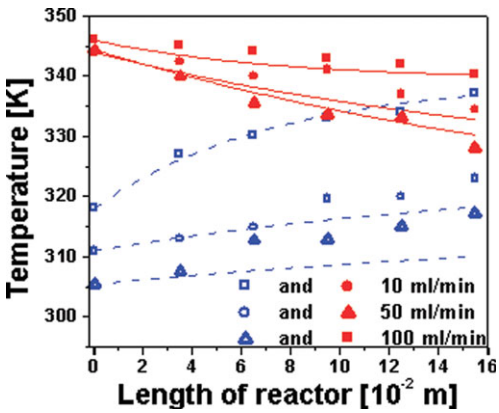

Figure 10. Axial temperature profile in the reactor part.

Experimental results vs. model predictions for different flow rates of the coolant (1.66, 8.33, $16.66{\cdot}10^{-7}$ m^3/s). Flow rate of the reaction mixture: $6.66{\cdot}10^{-7}$ m^3/s, available power: 163 W, symbols: experimental data, filled: reaction mixture (RM), open: coolant (C), Lines: modeling results, red lines: reaction mixture (RM), blue lines: coolant (C). [Color figure can be viewed in the online issue, which is available at wileyonlinelibrary.com.]

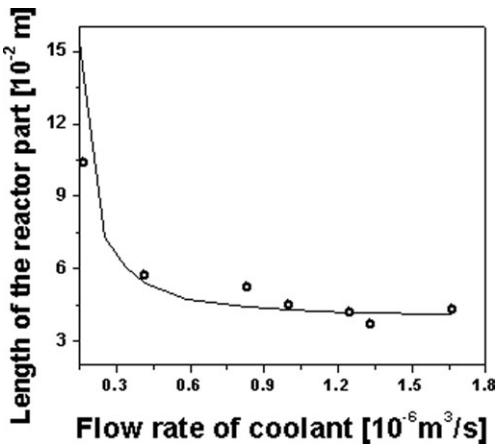

Figure 11. Validation of the length of the reactor part.

Symbols: experimental data, Line: modeling results.

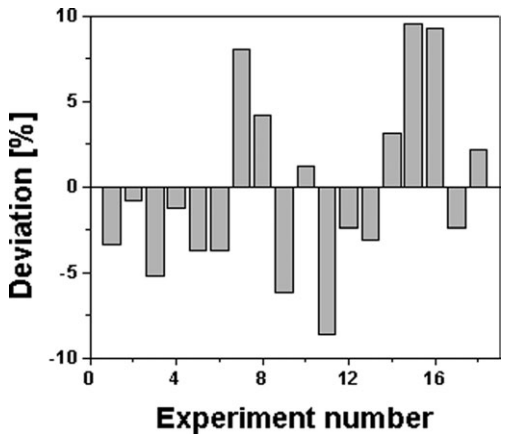

Figure 12. Deviation in heating efficiency from its average value of 96% calculated over several experiments.

Flow rate reaction mixture: 5–8.33·10^{-7} m^3/s, coolant: 8.33–2500·10^{-9} m^3/s, available power: 150–175 W.

part influenced the driving force for heat transfer in the reactor part (Figure 10). The lengths of the reactor part predicted by the heat-transfer model were found to be in good agreement with the experimental results (Figure 11). When the coolant flow rate was less than $1.66 \cdot 10^{-7}$ m^3/s, the complete reactor length of 0.155 m could be used for reaction, whereas it was about 0.043 m for a coolant flow rate above $1.25 \cdot 10^{-6}$ m^3/s. Thus, the optimized integration of heat has clearly lead to good prediction of the length of the reactor part which can essentially be used to conduct a reaction.

Validation of the Model with Chemical Reaction

The last step in this study was performing the esterification reaction in the catalyst bed downstream the microwave cavity part. As discussed in the previous section, the length of the reactor and, thus, the length of the catalyst bed were determined by the flow rate of the coolant. The expected conversion was calculated by incorporating Eq. 6 in the heat transfer model of the reactor part and compared with the experimental values. A maximum deviation of 2.5% has been found between the observed and the calculated conversions. This presumably was due to an inaccurate determination of the length of the reactor part or inaccurate GC analysis. In conclusion, these validation results demonstrate that microwave heating can be incorporated in millireactor flow processing in a controllable manner, giving predictable temperatures and conversions.

Microwave Heating Efficiency

To make microwave heating a justified heating technology, the energy efficiency has been calculated to check its viability when compared with conventional heating technologies. While heating the reaction mixture with microwaves, some of the power was reflected. The rest of the power was absorbed by the reaction mixture, and the coolant took up some of this energy by heat transfer. A part of this transferred heat got lost to the surroundings. However, considering usability the energy utilized only for heating the reaction mixture and the coolant (Q_{abs}, Eq. 7) was used to determine the efficiency of microwave heating by comparing it with the maximum amount of absorbed microwave energy that could be converted into heat (Q_{MW}, Eq. 1). The average heating efficiency (Eq. 8) of 96% with heat recovery (heat extracted by coolant Q_c) up to 2% was calculated from the available data of several experiments

$$Q_{abs} = \left(\dot{m} C_p \Delta T\right)_{RM} + \left(\dot{m} C_p \Delta T\right)_C \tag{7}$$

$$\text{Efficiency} = \frac{Q_{\text{abs}}}{Q_{MW}} 100\% \tag{8}$$

The deviation from the average value of the heating efficiency was found to be within 10% (Figure 12). This deviation was probably due to inaccurate temperature and reflective power measurements. Especially for the cases of high-flow rates of the coolant, 1 K error in the temperature measurement lead to an error of 8% in heating efficiency.

Nevertheless, having a heating efficiency of more than 90% is very important to prove microwave heating as a viable technology for industrial applications, at least for fine chemical synthesis. Usually, the electrical efficiency (conversion of electrical energy taken from the grid) of the standard marketed magnetrons like many other technologies such as resistive heating is in the range of 50–65%.[24] This brings the overall energy efficiency of such heating systems down to half ($90 \times 0.5 = 45\%$). Therefore, it is very important to carefully design a reactor system, which shall facilitate complete utilization of the produced (microwave) energy and provide heating efficiency above 90%. With our integrated reactor-heat exchanger approach, we prove that such a possibility exists to make microwave heating an attractive option for fine-chemical production scales of 1 kg/day (24 h periods).

Conclusions

Microwave heating can be beneficial over conventional heating (i.e., oil bath) especially with its clean and fast heating of polar reaction media at molecular level (volumetric heating). The major challenge of microwave heating being recognized as an alternative to conventional heating technology, however, lies in the possibility of taking microwave

batch processes to continuous operation. Therefore, a novel concept for continuous reactor operation under microwave heating is proposed where the temperature is maintained between a predefined low and high limit of operation by a cocurrent heat-exchanger by implementing a microwave transparent solvent, toluene, as a coolant. The heat transfer models for predicting the temperature profiles inside the microwave cavity as well as in the reactor part were developed and employed. The 2-D heat-transfer model of the microwave cavity predicted temperatures at the outlet of the microwave cavity with an accuracy of $\pm$ 3 K. However, future investigations are needed to understand the observed hot-spot formation inside the microwave cavity. The 1-D heat-transfer model for the reactor provided the lengths of the reactor packed with the catalyst bed for conducting the reaction between T_{max} (343 K) and T_{min} (338 K). Optimized integration of heat has clearly lead to good prediction of the length of the reactor part which was principally used to conduct a reaction. The observed conversions were found to be in good agreement with the predictions. Converting microwave energy into heat had an average efficiency of 96%. Thus, it can be concluded that application of microwave heating technology not only provides clean and fast heating at the molecular level, but also helps in performing a controlled and energy efficient continuous operation in a milli-reactor setup where temperatures and yields can be predicted accurately.

Outlook

Future work in this field focuses on benefits associated with fast heating, i.e., avoiding undesired side reactions during heating and controlled utilization of hot spots present on metallic catalytic surfaces for enhanced yields in copper catalyzed Ullmann ether synthesis.[25]

Acknowledgments

Authors would like to acknowledge DSM Research, Friesland-Campina, IMM, LioniX, Milestone s.r.l. and the Dutch Technology Foundation STW (project MEMFiCS GSPT-07974) for financial support. They would also like to acknowledge Mr. Erik Esveld and the Food and Biobased Research group (Wageningen University, The Netherlands) for putting the dielectric property measurement equipment at disposal.

Notation

Symbols

A = surface area perpendicular to flow, m^2
C_p = heat capacity, J/kg.K or J/mol.K
C_A = concentration of component A, mol/m^3
d = diameter, m
D_p = particle diameter, m
E = electric field intensity, V/m
E_a = activation energy, J/mol
f = microwave frequency, 2.45×10^9 Hz
F_v = volumetric flow rate, m^3/s
F = body force vector, N/m^3
$\Delta_r H_T^0$ = heat of reaction at reaction temperature (T = 343 k), J/mol
$\Delta_r H_{Ts=298K}^0$ = heat of reaction at room temperature, J/mol
k_{obs} = observed reaction rate constant, $m^3_{cat}/m^3_R.s$
k^v = volumetric reaction rate constant, 1/s
K_0 = frequency factor in Arrhenius equation
L = length of reactor, m
m = mass flow rate, kg/s
P = pressure, Pa
Q = microwave power, W
r'_A = rate of reaction, $mol/m^3_{cat}.s$
R = gas constant, 8.314 J/mol.K
T = temperature, K
t = time, s
U^* = overall heat-transfer coefficient, W/m^3 K
u = velocity, m/s
V = volume, m^3
W = volume of catalyst, m^3
X = conversion
z = direction

Greek letters

ε = voidage
ε' = dielectric constant
ε'' = dielectric loss
ε_0 = permittivity of free space, $8.85 \cdot 10^{-12}$ F/m
v = moles
μ = viscosity, Pa.s
ρ = density, kg/m^3
λ = thermal conductivity of solids, W/m.K
k = thermal conductivity of liquids, W/m.K

Subscripts

C = coolant
RM = reaction mixture
R = reactor
cav = Cavity
abs = absorbed heat
MW = microwave
loss = loss to the surroundings
f = formation
cat = catalyst
r = reaction
T = temperature
s = surroundings
i = component number

Literature Cited

1. Gedye R, Smith F. The use of microwave ovens for rapid organic synthesis. *Tetrahedron Lett*. 1986;27:279–282.
2. Damm M, Glasnov NT, Kappe OC. Translating high-temperature microwave chemistry to scalable continuous flow processes. *Org Process Res Dev*. 2010;14:215–224.
3. Plazl I, Pipus G, Koloini T. Microwave heating of the continuous flow catalytic reactor in a nonuniform electric field. *AIChE J*. 1997;43:754–760.
4. Chemat F, Poux M, Di Martino JL, Berlan J. A new continuous-flow recycle microwave reactor for homogeneous and heterogeneous chemical reactions. *Chem Eng Technol*. 1996;19:420–424.
5. Glasnov NT, Kappe OC. Microwave-assisted synthesis under continuous-flow conditions. *Macromol Rap Com*. 2007;28:395–410.
6. Chemat F, Esveld E, Poux M Di-Martino LJ. The role of selective heating in the microwave activation of heterogeneous catalysis reactions using a continuous microwave reactor. *J Microwave Power Electromagn Energy*. 1998;33:88–94.
7. Baxendale IR, Griffiths-Jones MC, Ley VS, Tranmer KG. Microwave-assisted Suzuki coupling reactions with an encapsulated palladium catalyst for batch and continuous-flow transformations. *Chem Eur J*. 2006;12:4407–4416.
8. Cecilia R, Kunz U, Turek T. Possibilities of process intensification using microwaves applied to catalytic microreactors. *Chem Eng Process*. 2007;46:870–881.
9. Roberts AB, Strauss RC. Towards rapid, 'green' predictable microwave-assisted synthesis. *Acc Chem Res*. 2005;38:653–661.
10. Esveld E, Chemat F, van Haveren J. Pilot scale continuous microwave dry-media reactor - Part 1: design and modeling. *Chem Eng Technol*. 2000;23:279–283.
11. Esveld E, Chemat F, van Haveren J. Pilot scale continuous microwave dry-media reactor - Part II: Application to waxy ester production. *Chem Eng Technol*. 2000;23:429–435.
12. Kabza GK, Chapados RB, Estwicki EJ, McGrath LJ. Microwave-induced esterification using heterogeneous acid catalyst in a low dielectric constant medium. *J Org Chem*. 2000;65:1210–1214.
13. Strauss RC. Microwave-assisted reactions in organic synthesis - are there any nonthermal microwave effects? Response to the highlight by N. Nuhnert. *Angew Chem Int Ed*. 2002;41:3589–3590.

14. Patil NG, Rebrov EV, Benaskar F, Esveld E, Sturm GSJ, Meuldijk J, Hessel V, Hulshof LA, Schouten JC. Optimization of heating efficiency under monomode microwave heating for efficient utilization of energy in microwave-assisted flow processing, *J Microwave Power Electromagn Energy* (submitted).
15. Pipus G, Plazl I, Koloini T. Esterification of benzoic acid in microwave tubular flow reactor. *Chem Eng J*. 2000;76:239–245.
16. Wilson SN, Sarko RC, Roth PG. Development and applications of a practical continuous flow microwave cell. *Org Process Res Dev*. 2004;8:535–538.
17. Hoogenboom R, Wilms AFT, Schubert SU. Microwave irradiation - a closer look at heating efficiencies. *Polym Preprints*. 2008;49:930–931.
18. Herrero MA, Kremsner JM, Kappe CO. Nonthermal microwave effects revisited: on the importance of internal temperature monitoring and agitation in microwave chemistry. *J Org Chem*. 2008;73:36–47.
19. Fogler HS. *Elements of Chemical Reaction Engineering*. 4th ed. Upper Saddle River, NJ, US: Pearson Education International; 2006.
20. Lide DR. *CRC Handbook of Chemistry and Physics*. Boca Raton: Taylor & Francis group, 2000.
21. Shah KR, London LA, eds. *Laminar flow forced convection in ducts: A source book for compact heat exchanger analytical data*. New York: Academic Press; 1978.
22. Metaxas CA, Meredith JR. *Industrial Microwave Heating*. London, U.K: Peter Peregrinus ltd; 1983.
23. Kirbaslar IS, Baykal BZ, Dramur U. Esterification of acetic acid with ethanol catalyzed by an acidic ion-exchange resin. *Turk J Eng Environ Sci*. 2001;25:569–577.
24. Moseley JD, Kappe CO. A critical assessment of the greenness and energy efficiency of microwave-assisted organic synthesis. *Green Chem*. 2011;13:794–806.
25. Benaskar F, Engels V, Patil NG, Rebrov EV, Meuldijk J, Hessel V, Hulshof LA, Jefferson DA, Schouten JC, Wheatley AEH. Copper(0) in the Ullmann heterocycle-aryl ether synthesis of 4-phenoxypyridine using multimode microwave heating. *Tetrahedron Lett*. 2010;51:248–251.
26. Toukoniitty B, Mikkola JP, Eranen K, Salmi T, Murzin DY. Esterification of propionic acid under microwave irradiation over an ion-exchange resin. *Catal Today*. 2005;100:431–435.
27. Teo HTR, Saha B. Heterogeneous catalysed esterification of acetic acid with isoamyl alcohol: kinetic studies. *J Catal*. 2004;228:174–182.

Appendix A: Heat of Reaction

The heat of reaction at 343 K was calculated solving following equations

$$\Delta_r H_T^0 = \Delta_r H_{T_s=298K}^0 + \int_{T_s}^{T} \Delta_r Cp^0 dT \tag{A1}$$

$$\Delta_r H_{T_s=298K}^0 = \sum \upsilon_i * \Delta_f H_{i,T_s=298K}^0 \tag{A2}$$

$$\Delta_r Cp^0 = \sum \upsilon_i * Cp_i^0 \tag{A3}$$

$$Cp_i^0 = a_0 + a_1 * T + a_2 * T^2 + a_3 * T^3 + a_4 * T^4 \tag{A4}$$

Solving Eqs. A.1–A.4 with the data of Table A1 gave the heat of reaction of −2,438 J/mol. Thus the reaction is slightly exothermic.

Appendix B: Pressure-Drop Calculations

The pressure drop over a packed bed can be computed by using the Ergun equation (Eq. B1). The pressure drop was calculated for the longest possible catalyst bed length of 0.155 m

$$\frac{dP}{dz} = -\frac{150^* u^* \mu}{D_p^2} * \frac{(1-\varepsilon)^2}{\varepsilon^3} + 1.75 \frac{\rho^* u^2}{D_p} * \frac{(1-\varepsilon)}{\varepsilon^3} \tag{B1}$$

The pressure drop was calculated by using physical properties of the system (Table B1) to be $0.18 \cdot 10^5$ Pa.

Appendix C: Reaction Rate Constant

In this work, the solid acid catalyzed esterification reaction[6,9,11,15] of ethyl acetate formation from acetic acid and ethanol was chosen as a model reaction.[23] This is a simple reaction with well-understood kinetics.[26,27] The reaction equation is presented in Scheme 1. In order to increase the conversion for this equilibrium limited reaction a five-fold excess of ethanol was chosen because of its dielectric properties. This excess made the reaction to obey a pseudo first-order rate law. The effect of temperature on the reaction rate constant and the effect of catalyst loading on the conversion were determined. The effect of temperature was determined to establish the activation energy. The effect of catalyst loading was needed to calculate the volumetric reaction rate constant (independent of the catalyst loading), which was used later for reaction modeling.

Experimental setup and procedure

The used setup for the kinetic experiments is schematically depicted in Figure C1. The experiments were performed in a batch reactor. An oil bath was used to achieve the reaction temperature and to keep it constant.

The batch reactor (three-necked round-bottom flask) had a capacity of $50 \cdot 10^{-6}$ m^3 and was equipped with a reflux condenser to prevent any losses of the reactants by evaporation. Samples were taken via one of the necks. The reaction mixture was magnetically stirred at 750 rpm. The reaction vessel was kept at a constant temperature in a stirred-constant temperature oil bath, where the temperature could be monitored and adapted manually with a thermocouple. Chemicals and catalysts used for this study were as explained in the experimental section. Experiments were carried out at a molar ratio of ethanol to acetic acid of 5:1 at different temperatures (323 to 343 K, at 20 wt % dry catalyst loading), and

Table A1. Thermodynamic Data of Reaction Components for Heat of Reaction Calculations

Component	υ_i	$\Delta_f H_{i,Ts=298K}$ kJ/mol	Cp_i				
			a_0	$a_1 \times 10^{-4}$	$a_2 \times 10^{-5}$	$a_3 \times 10^{-8}$	$a_4 \times 10^{-11}$
Acetic acid	−1	−484.3	4.38	−24.0	6.76	−8.76	2.69
Ethanol	−1	−277.6	4.40	6.28	5.55	−7.02	3.48
Ethyl acetate	1	−479.3	10.23	−149	13.0	−15.7	6.00
Water	1	−285.8	4.40	−41.9	1.41	−1.56	0.663

Table B1. Physical Properties of System and Components for Pressure-Drop Calculations by Ergun Equation

Variable	Value	Description
ε	0.2	Porosity, [m^3_{cat}/m^3_R]
D_p	$7.50 \cdot 10^{-4}$	diameter of particle, [m]
μ	$4.87 \cdot 10^{-4}$	Viscosity, [Pa.s]
z	$1.55 \cdot 10^{-1}$	length of the bed, [m]
u	$9.4 \cdot 10^{-2}$	superficial velocity, [m/s]
rho	770	Density, [Kg/m^3]

different catalyst loadings (5 to 20 wt % at 343 K). The volume of the reaction mixture was $25 \cdot 10^{-6}$ m^3 for all experiments. The reaction mixture was charged to the reactor, and the catalyst was added when the reaction mixture has reached the desired reaction temperature. The liquid samples were analyzed by gas chromatography by following the procedure described in the experimental section.

Results

Figure C2 shows a typical concentration time history for the reactants and products during the reaction.

Effect of temperature

The effect of temperature on the conversion of the limiting reactant, i.e., acetic acid, was checked by calculating $-\ln(C_A/C_{A0})$ over time, this gave a linear line, as expected for a (pseudo) first-order reaction with slope being the observed reaction rate constant (k_{obs}). The ln k_{obs} showed a linear dependence over the reciprocal of the temperature, see Figure C3.

The activation energy (E_a) and frequency factor (K_0) were calculated to be 53,500 J/mol and $2.65 \cdot 10^6$ s^{-1}, respectively, by applying the Arrhenius equation (Eq. C1).

$$k_{obs}(T) = K_0 e^{-\frac{E_a}{RT}} \tag{C1}$$

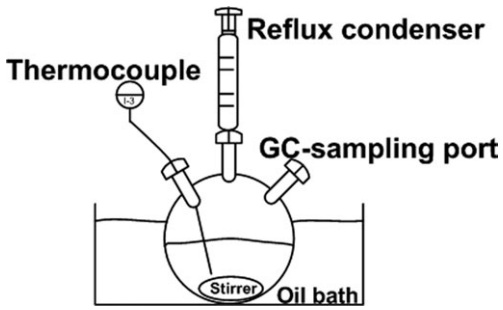

Figure C1. Schematic of the setup used for kinetic experiments.

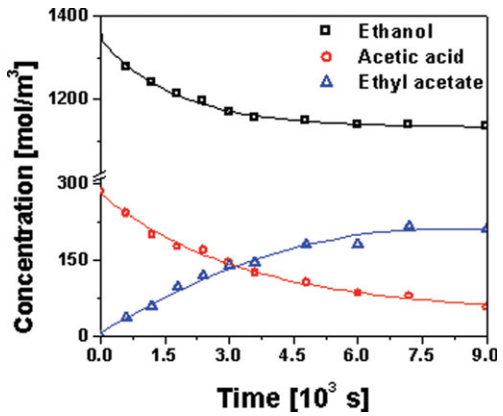

Figure C2. Typical concentration-time profile of the esterification reaction.

Catalyst loading: 5%, Temperature: 343 K, Agitation speed: 750 rpm. [Color figure can be viewed in the online issue, which is available at wileyonlinelibrary.com.]

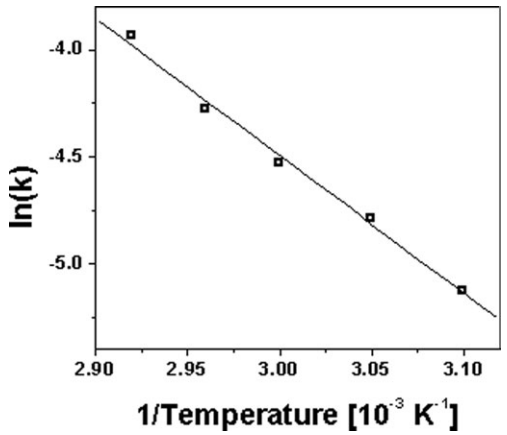

Figure C3. Effect of temperature on the reaction rate coefficient of the esterification reaction.

Catalyst loading: 20%, Reaction volume: $2.5 \cdot 10^{-5}$ m^3, Agitation speed: 750 rpm.

Effect of catalyst loading

The effect of the catalyst loading on k_{obs} at 343 K was determined. A linear dependence was found as shown in Figure C4.

The observed reaction rate constant was corrected for the catalyst loading by equating Eqs. C2 and C3. The first-order rate coefficient based on the reaction rate per unit volume of catalyst (k^V) of $3.28 \cdot 10^{-3}$ s^{-1} was calculated from k_{obs} using Eq. C5

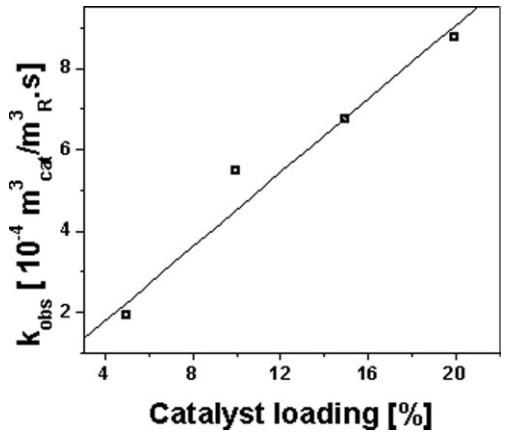

Figure C4. Effect of Catalyst loading on the reaction rate coefficient (k_{obs}) of the esterification reaction.

Temperature: 343 K, Reactor volume: $2.5 \cdot 10^{-5}$ m^3, Agitation speed: 750 rpm.

$$V_R \frac{dC_A}{dt} = k_{\text{obs}} C_A V_R \tag{C2}$$

$$V_R \frac{dC_A}{dt} = k^V C_A V_{cat} \tag{C3}$$

Therefore

$$k^V V_{\text{cat}} = k_{\text{obs}} V_R \tag{C4}$$

$$k^V = \frac{k_{\text{obs}} V_R}{V_{\text{cat}}} \left[\frac{1}{s}\right] \tag{C5}$$

Manuscript received May 13, 2011, and revision received Nov. 18, 2011.